Designing the Printed Dog-Borne Dipole Structure

Nataša Nešic[1], Bratislav Milovanovic[2], Nebojša Donèov[3], Vanja Mandric-Radivojevic[4], Slavko Rupcic[1]
[1]College of Applied Technical Sciences Niš
Aleksandra Medvedeva 20, Niš 18000, Serbia
{natasa.bogdanovic@vtsnis.edu.rs}

[2]University of Singidunum, Danijelova 32
Belgrade 11000, Serbia
{bmilovanovic@singidunum.ac.rs}

[3]University of Niš, Aleksandra Medvedeva 14
Niš 18000, Republic of Serbia
nebojsa.doncov@elfak.ni.ac.rs

[4]Osijek 31000, Croatia
{vanja.mandric@etfos.hr, rupcic@etfos.hr}

ABSTRACT: *In this work we addressed the approach for designing a printed dog-bone dipole antenna. The results arrived are related to the numerical and experimental models of the printed structure. We study the models of the enclosure so as to develop the protection function. Further we analyse the structure on values of shielding effectiveness. To get the best results we changed the three parallel positions inside the enclosure.*

Keywords: Aperture, Enclosure, Shielding Effectiveness, Dogbone Dipole Structure, Monopole Antenna, TLM Wire Method

Received: 18 August 2020, Revised 18 November 2020, Accepted 28 November 2020

1. Introduction

At resonant frequencies, the shielding metal enclosure can indicate very low or even negative values of the shielding effectiveness (SE) [1]. Consequently, the resonant frequencies of the enclosure can be critical since they might compromise the useful frequency range in which electromagnetic (EM) shielding is provided. Therefore, several techniques were implemented to improve the shielding properties. For instance, in [2] an extra aperture as a matched load instead of a shorted waveguide was proposed by using TLM (Transmission Line Matrix) method. Paper [3] combined MoM and FEM methods for EM field distribution to determine the effect of the aperture size of a loaded enclosure with PCB(s) inside. Also, SE can be improved by using conductive foam, or absorbers [4], [5]. Furthermore, the composite materials based on nanotechnology [6], metamaterial structure [7] and a frequency-selective surface [8] can be employed as damping techniques. The enclosure can be coated with composite material or can be made of that material [9].

More related to this work, in [10] a simple strategy was proposed to suppress the first resonance in a metal enclosure by putting small antenna elements with loaded resistance. It was shown that placing a small dipole or loop antenna structure on

the enclosure wall opposite to the enclosure aperture can improve the enclosure SE. The effective length of this printed structure was chosen to match the enclosure's first resonant frequency. Numerical study, based on this research, was carried out in [11], to further investigate this strategy.

In this paper, the impact of the printed dipole dog-bone antenna inserted in the shielding metal enclosure with a rectangular aperture is considered both numerically and experimentally from the viewpoint of the shielding effectiveness of enclosure. The dog-bone antenna structure, with the dimensions designed to influence the first enclosure resonance, is printed on an epoxy substrate which is placed inside the enclosure in three positions parallel to the aperture wall. Numerical and experimental SE results of the enclosure are obtained by using a receiving-monopole antenna.

2. Numerical TLM Wire Model

Anumerical modeling technique, called the TLM method [12], is employed in this paper. The TLM method has been enhanced with a number of different compact models to allow an efficient modelling of EM important features [12]-[14]. For modelling an antenna inside enclosure whose purpose is to measure the EM field level and distribution, the compact wire model is the most appropriate. It is based on wire segment incorporated into the Symmetrical Condensed Node (SCN). The SCN with wire segment is running in z-direction is shown in Figure 1. The impedances of additional wire network link and short-circuit stub lines depend on used space and time-step discretization, and also on per-unit length wire capacitance and inductance [14]. Two-way coupling between signal in the *z*- directed wire circuit and external EM field described by pulses in transmission line network of SCN (marked bold in Figure 1) is achieved through points A and B. In considered case, the wire is connected to the ground via resistor R. The induced current on the wire, due to external EM field, generates voltage on the resistor R, loaded at wire base, allows measuring the level of EM field.

The considered metal enclosure is shown in Figure 2. It is rectangular, with internal dimensions of (300 x 400 x 200) mm^3 and an aperture of dimensions (50 x 10) mm^2 is positioned symmetrically around the center on the frontal wall. Material from which the enclosure is made of is copper. Thickness of the enclosure walls is $t = 2\ mm$, while the frequency range of interest is from 400 *MHz* to 2 *GHz*. The monopole-receiving antenna with radius of 0.1 mm and length of 100 mm, made of copper, is placed in the middle of the enclosure. Excitation source is vertically polarized incident plane wave. The characteristics of the enclosure, i.e., its geometry, dimensions and aperture shape, the excitation source, the monopole antenna position and its length are assumed to be as in [1].

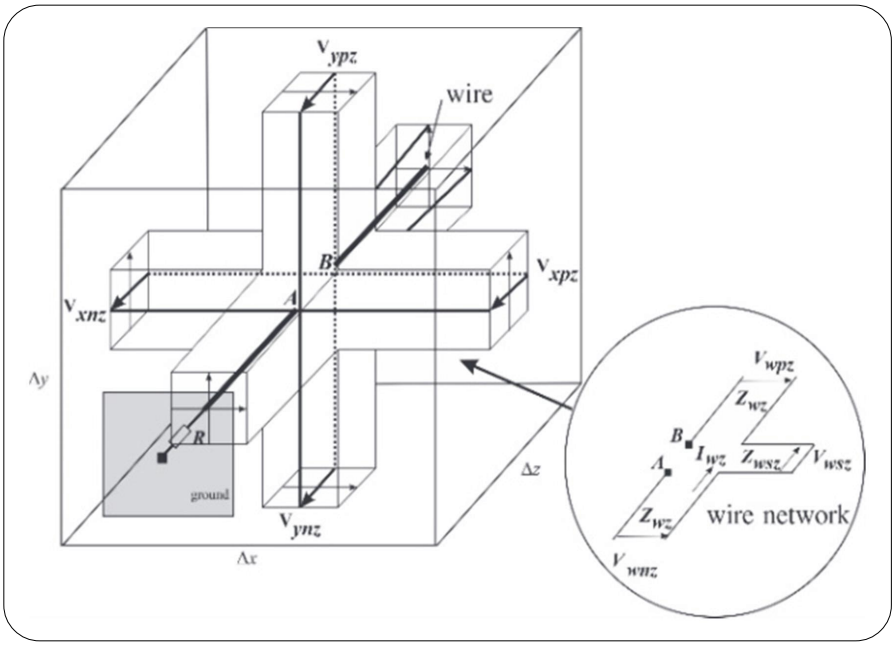

Figure 1. The SCN wire segment in *z*- direction is terminated with the resistor *R* to the ground plane [1]

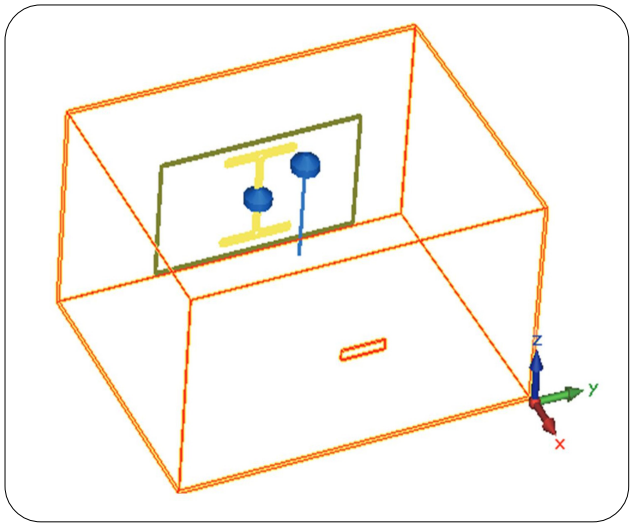

Figure 2. Anumerical shielding metal enclosure with aperture has the printed dog-bone dipole structure and receiving-monopole inside

The dog-bone antenna structure, with dimensions which are designed to influence the first enclosure resonance, is printed on an epoxy substrate which is placed inside the enclosure in three positions parallel to the aperture wall. The effective length of the printed dog-bone dipole structure corresponds to the first resonant frequency of the enclosure [10], which occurs at 625 MHz [1]. The effective length of the printed dipole is l = 240 mm, with strip width and thickness of 5 *mm* and 35 μm, respectively. The dog-bone dipole is loaded with a resistor R. The epoxy substrate has dimensions of (115 x 230) mm^2 with thickness of 1.6 mm, and relative permittivity $\varepsilon_r = 4$.

3. Experimental Procedure and Physical Model

According to the numerical model, the physical one is realized with the same internal dimensions and material. The dog-bone dipole is realized on the epoxy substrate by using photolithographic technique. Figure 3 illustrates the physical enclosure which is used in experimental measurements, with the monopole-receiving antenna and dog-bone dipole inside, without the aperture wall. The printed dog-bone structure has a SMD resistor of $R = 47\Omega$ due to the practical reasons.

The measurement processes are performed in a semi-anechoic room by using the spectrum analyzer with tracking generator and the SPIKE Software for computer with Intel processor i5, as depicted in Figure 4. A transmitting dipole antenna was a Vivaldi dipole antenna while a receiving antenna was an in-house monopole antenna.

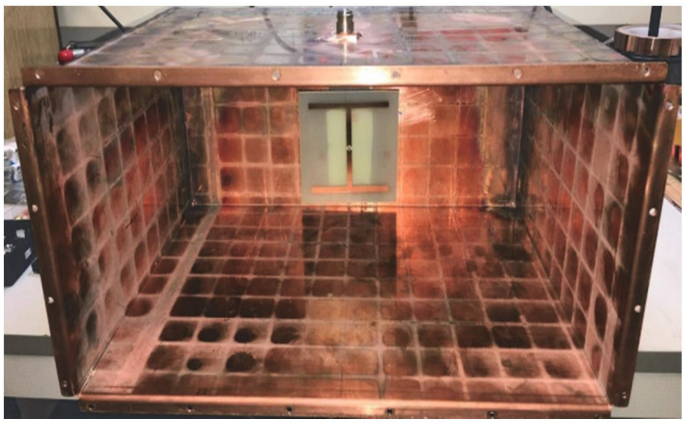

Figure 3. The dog-bone dipole structure in physical metal enclosure

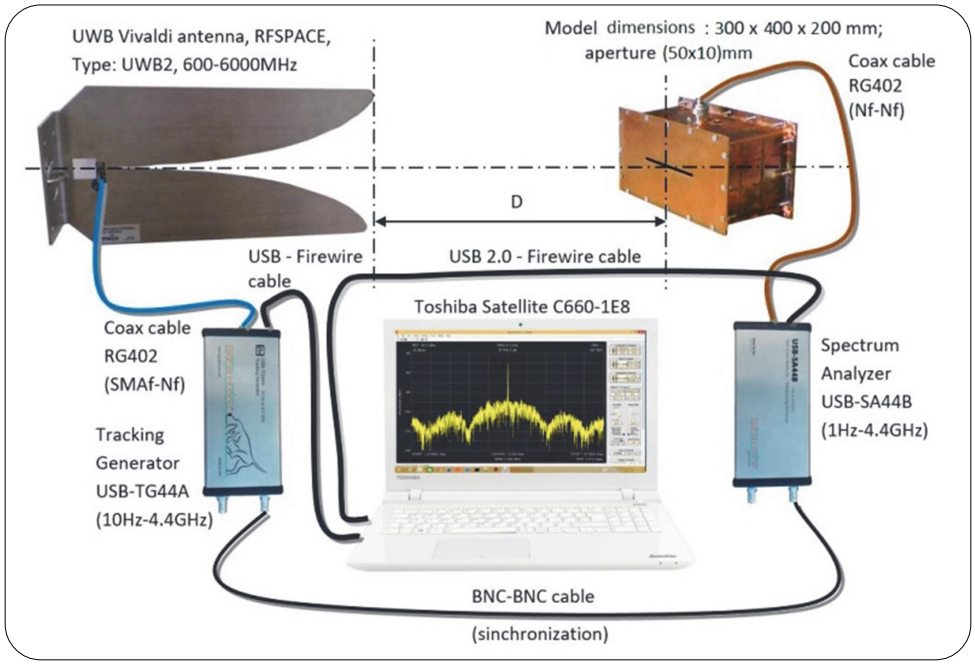

Figure 4. The measuring configuration used in a semi-anechoic room

4. Discussion of Numerical and Experimental Results

In this section, we discuss the impact of printed dog-bone dipole structure in enclosure on the SE value at the first enclosure resonance. The printed structure is placed in three different positions inside the enclosure, at 150 *mm*, 100 *mm* and 50 *mm* from the enclosure center, respectively. Both numerical and experimental analyses are conducted in order to improve effectiveness of the enclosure.

In the first scenario, the epoxy substrate with the printed dog-bone structure is placed in the center of the enclosure wall, opposite to the aperture wall of the considered model (see Figure 3). The enclosure is excited with an incident plane wave vertically polarized in *z*-direction by using the Vivaldi dipole as a transmitting antenna, while in the center of the enclosure the monopole-receiving antenna is placed. Figure 5 illustrates the comparative analysis of the numerical and experimental results for the whole observed frequency range. The numerical curves results are labelled as *Empty_sim* for the empty enclosure, *Monopole_sim* for the enclosure with monopole-receiving antenna and Dog-bonefr1_150mm for the case with dog-bone on the wall opposite to the aperture wall, in presence of the receiving-monopole in the center. The experimental analyses are labelled: *Monopole_meas* for the case with receiving in-house monopole, *Dog-bone fr1_150mm*_measis related to receiving in-house monopole and the printed dog-bone structure, as presented in Figure 3. It can be observed that both simulated and measured results have a very good match. A narrow frequency range, from 400 MHz to 800 MHz, is shown in Figure 6 since it is important for observing the SE values occurred at the first resonance of the enclosure. It is evident that the monopole-receiving antenna inside enclosure creates some perturbation. Consequently, the position of the first resonance is shifted toward the lower frequencies in comparison to the empty enclosure, which is analyzed in detail in [1]. It can be observed that the SE results for the first resonance is higher for about 20 dB in comparison to the empty enclosure. In Table 1, the SE values at the first resonant frequencies are provided for all considered cases.

The second scenario is conducted for the numerical model with the same printed dog-bone structure which is now shifted 50 mm from the internal enclosure wall toward the enclosure center. In other words, the dog-bone structure is placed 100 mm from the center of enclosure to the wall which is opposite to the aperture wall. Figure 7 illustrates the numerical SE curves obtained for Dog-bone fr1_100mm and *Monopole_sim* are quite similar. For the experimentally measured results, the SE measured curve for the second dogbone scenario is shifted toward lower frequencies, at the first resonant frequency, in comparison to the *Monopole_meas* and the first dog-bone scenario. Also, the SE values at the first resonance and around resonance increase in contrast to the resonance of the empty enclosure.

Dog-bone structure	fr1_sim [MHz]	fr1_meas [MHz]	SE_sim[MHz]	SE_meas [dB]
fr1_150mm	582.025	575.923	26.11	22.99
fr1_100mm	578.631	559.894	25.74	27.87
fr1_50mm	523.286	536.091	35.92	29.35
Empty	624.365	-	-2.22	-
Monopole	583.045	582.632	24.41	20.99

Table 1. The se values at the first enclosure resonance

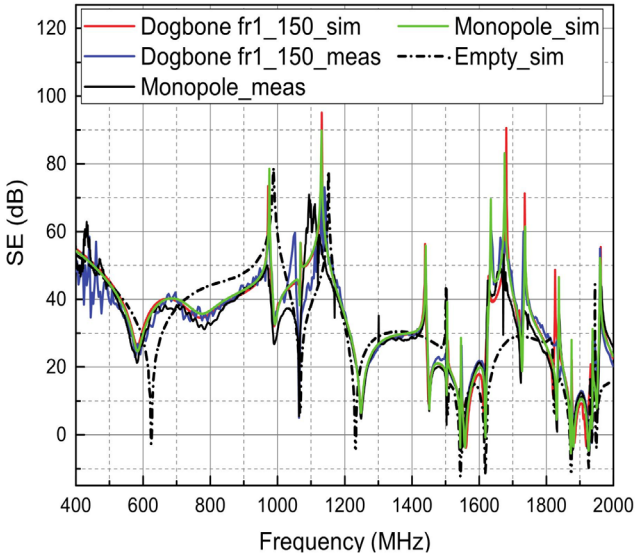

Figure 5. The SE of enclosure with a printed dog-bone structure placed at 150mm from the enclosure center and with receiving monopole

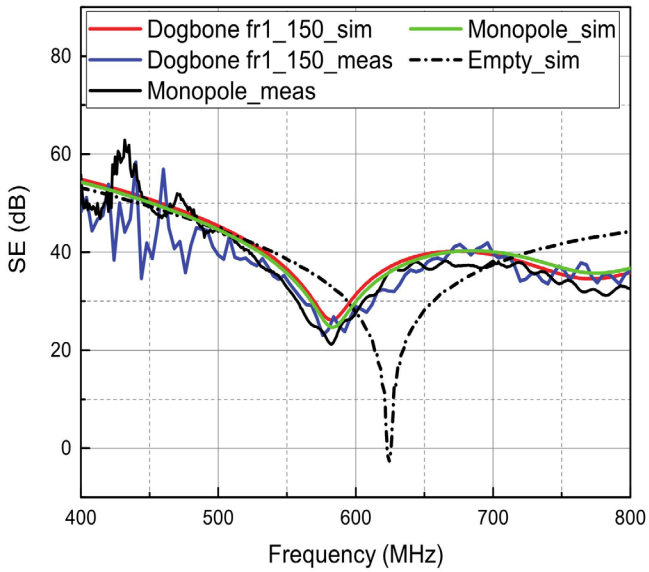

Figure 6. The frequency range around the first resonant frequency for scenario as in Figure 5

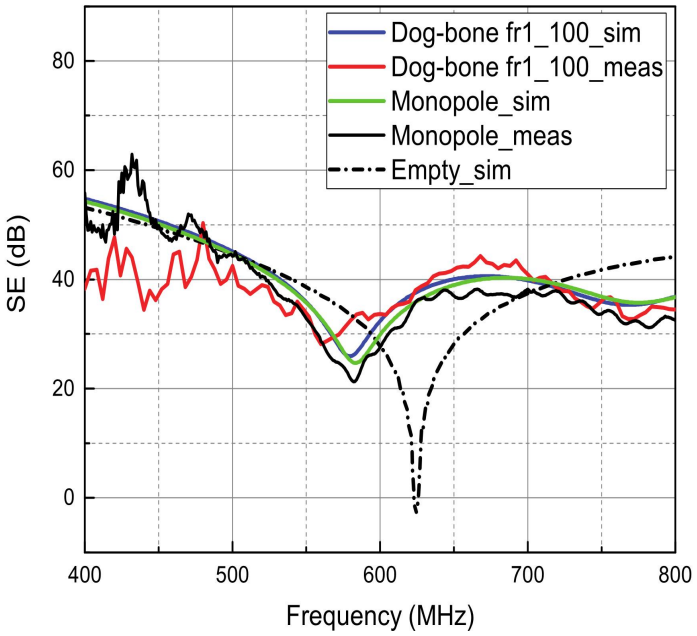

Figure 7. The first resonance SE peaks for the second dog-bone scenario, enclosure with monopole antenna and the empty enclosure

In the third scenario, we put the printed dog-bone dipole at position of 50 mm from the enclosure centermrc4. In Figure 8 it can be observed that the third dog-bone dipole gives the most significant improvement in comparison to other two scenarios.

Figure 9 gives the measured SE characteristics for the three dog-bone dipole scenarios. Table I shows the values of the first resonant frequencies and the amplitudes for all three scenarios. It is clear that the third scenario has the most prominent suppression. The improvement in the suppression of the SE amplitude at the resonance is significant, (35.92-(-2.22)) dB = 38.14 dB for *Dog-bone fr1_50* compared to the empty enclosure, and the level of (35.92-24.41) dB = 11.51 dB for *Dog-bone fr1*_50 compared to the enclosure with monopole. It should be noted that these data are given for numerical analysis. In addition, the measurements related to dog-bone structure are consistent with the corresponding numerical analyzes and, according to the perturbation theory, this is expected impact of the body placed into the resonator.

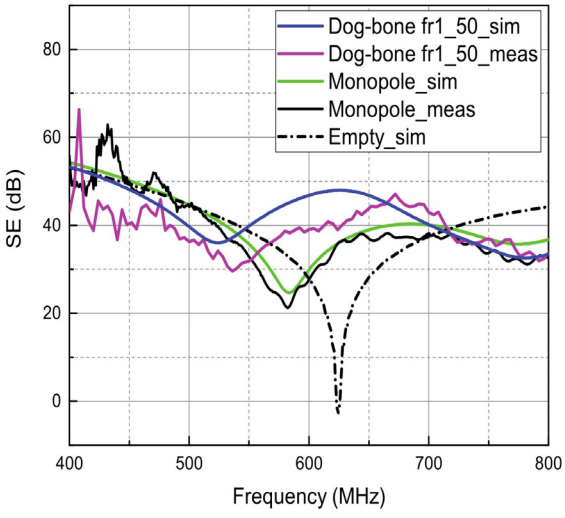

Figure 8. The first resonance SE peaks for the third dog-bone scenario, enclosure with monopole antenna and the empty enclosure

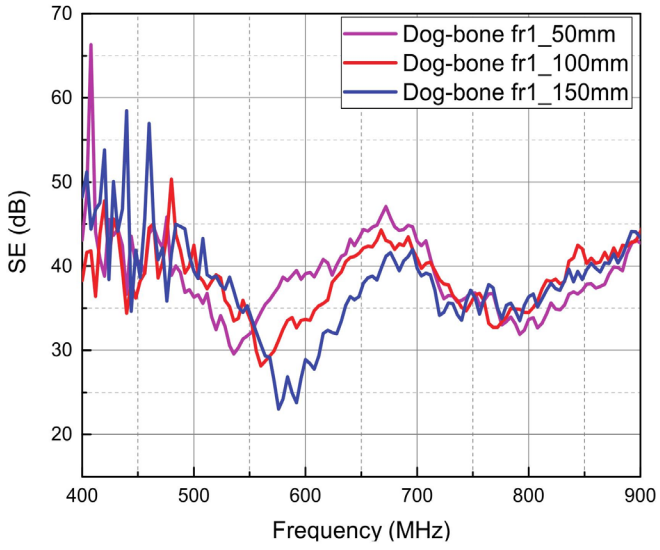

Figure 9. The measured first resonance SE peaks for the three dog-bone scenarios in the enclosure

5. Conclusion

To increase the SE level of the shielding enclosure, especially at the first resonance frequency, a printed dog-bone structure, with dimensions which are designed to influence the first enclosure's resonance, is put inside the enclosure. It has been shown that this structure may improve the SE around 30dB. Also, there might be a resonance frequency shift of around 90MHz.Further research can be related to finding the appropriate printed dipole structure with dimensions and shape which can be adequate for suppressing the first three enclosure resonances. Also, we will analyze the case for another receiving antenna which creates less perturbation of EM field distribution inside an enclosure, e.g. a dipole antenna [1].

Acknowledgement

This work has been partially supported by the Ministry for Education, Science and Technological Development of Serbia; projectnumberTR32052, by the EUROWEB+ project and by the COST IC 1407 Action.

References

[1] Nešiæ, N. J., Donèov, N. S. (2016). Shielding Effectiveness Estimation by using Monopole-receiving Antenna and Comparison with Dipole Antenna, Frequenz DeGruyter, no. 5- 6, DOI 10.1515/freq-2015-0203, p. 1-11.

[2] Bahadorzadeh, M., Lotfi-Neyestanak, A. A. (2012). A Novel and Efficient Technique for Improving Shielding Effectiveness of a rectangular Enclosure using Optimized Aperture Load, Elektronika ir Elektrotechnika, 18 (10) 89-92.

[3] Yenikaya, S., Yenikaya, G. (2011). Electromagnetic Coupling Analysis of Signal throught Aperture Perforated in a Loaded Shielding Enclosure Using Hybrid MoM/FEM, *Int. Journal of Basic & Applied Sciences IJBAS-IJENS*, 11 (6) 81- 86.

[4] Kumar, R., Dhakate, S. R., Saini, P., Mathur, R. B. (2013). Improved Electromagnetic Interference Shielding Effectiveness of Light Weight Carbon Foam by Ferrocene Accumulation, *The Roy. Soc. of Chem*. 2013: RSC Advances, vol. 3, p. 4145-4153.

[5] Luo, X., Chung, D. D. (1999). Electromagnetic Interference Shielding Using Continuous Carbon-Fiber Carbon-Matrix and Polymer-Matrix Composites, Elsevier Science:Composites: Part B , vol. 30, p. 227-231.

[6] Gupta, T. K., Singh, B. P., Mathur, R. B., Dhakate, S. R. (2014). Multi-Walled Carbon Nanotube–Graphene–Polyaniline Multiphase Nanocomposite with Superior Electromagnetic Shielding Effectiveness, *The Royal Society of Chemistry* 2014: Nanoscale, vol. 6, p. 842-851.

[7] Costa, F., Genovesi, S., Monorchio, A., Manara, G. (2000). A Circuit-based Model for the Interpretation of Perfect Metamaterial Absorbers, IEEE Trans. on Antennas and Propagation, 63 (3) 1201 - 1209.

[8] Munk, B. A. (2000). Frequency Selective Surfaces Theory and Design, New York: John Wiley and Sons, Inc.,.

[9] Ameli, A., Jung, P. U., Park, C. B. (2013). Electrical Properties and Electromagnetic Interference Shielding Effectiveness of Polypropylene/Carbon Fiber Composite Foams, Elsevier: Carbon, vol. 60, p. 379-391.

[10] Paul, J., Greedy, S., Wakatsuchi, H., Christopoulos, C. (2011). Measurements and Simulations of Enclosure Damping Using Loaded Antenna Elements, 10th Int. Symp. on EMC, p. 676– 679, York.

[11] Cvetkoviæ, T. (2015). Numerical Characterization of Shielding Effectiveness of an Enclosure with Apertures Based on Coupling with the Wire Structures (in Serbian), Niš: Doctoral disertation, *Faculty of Electonic Engineerin*g, p. 107- 119.

[12] Christopoulos, C. (1995). The Transmission-Line Modelling (TLM) Method, New Jersey: IEEE Press in assoc. with Oxford University Press, Piscataway.

[13] Wlodarczyk, A. J., Trenkiæ, V., Scaramuzza, R., Christopoulos, C. (1998). A Fully Integrated Multiconductor Model for TLM, IEEE Trans. of MTT, 46 (12) 2431-2437.

[14] Trenkiæ, V., Wlodarczyk, A. J., Scaramuzza, R. (1999). A Modelling of Coupling between Transient Electromagnetic Field and Complex Wire Structures, *Int. Journal of Num. Modelling*, 12 (4) 257-273.